rhodesiae 5 株、*M. gadium* 5 株、*M. nonchromogenicum* 5 株、*M. neoaurum* 7 株、*M. gordonae* 6 株、*M. szulgai* 6 株、及び *M. smegmatis* 8 株）のコロニーをテンプレートとしたPCR反応と電気泳動を行った。また、テンプレートとして用いた抗酸菌の菌種と今回行った鑑別法の結果が一致しなかった株については、市販のキット（抗酸菌同定キット：極東製薬工業）を用いて同定をやり直した。さらに結核菌群を特異的に検出するため、結核菌群のゲノム上にのみ存在している Rv3786c 遺伝子に対応するプライマーの設計を行った。作成したプライマーを用いて、結核菌群と非結核抗酸菌のゲノムとコロニーをそれぞれテンプレートとしたPCR反応と電気泳動を行った。

倫理面への配慮　本研究は、バイオセーフティーレベルに応じた該当実験室（P2 レベルまたは P3 レベル）で行った。実験を行う際には研究所内の安全講習を受講するとともに、実験計画について安全委員会の承認を受けている。また、大臣確認実験を必要とする実験（組換え DNA 実験）については、必要書類を文部科学省に提出し認可されている。実際の実験では、関連法令を遵守した上で、安全性等に十分に配慮して行った。

C. 研究結果

1. 抗酸菌に特異的な細胞壁構造に関与する新規遺伝子の同定

抗酸菌のゲノム情報を基に、結核菌のゲノム上でリポアラビノマンナンの生合成に関与していることが既に報告されている遺伝子群（結核菌のゲノム上で Rv2610c、Rv2611c、及び Rv2612c 遺伝子）と同じオペロン上に存在している２つの機能未知遺伝子（結核菌のゲノム上で Rv2609c 遺伝子と Rv2613c 遺伝子）、並びに細胞壁の構造に関与していると考えられている遺伝子群（結核菌のゲノム上で Rv3781、Rv3782、及び Rv3783 遺伝子）と同じ発現調節を受けている３つの機能未知遺伝子（結核菌のゲノム上で Rv3779、Rv3780、及び Rv3785 遺伝子）を細胞壁の合成に関与している遺伝子として選定した。なお、５つの遺伝子は全て抗酸菌において高度に保存されていた。*M. smegmatis* mc^2 155 を用いて、相同組換えによって選定した遺伝子をそれぞれ破壊した株の作成を行った結果、これまでに MSMEG2936 遺伝子（結核菌では Rv2609c 遺伝子に相当）を破壊した株（破壊株）が得られた。作成した破壊株のコロニー形態は、野生株のコロニー形態で見られる Rough 型ではなく、Smooth 型を示した（Fig. 1 A, B）。一方、破壊株中で結核菌由来の Rv2609c 遺伝子（MSMEG2936 遺伝子に相当）を発現させた相補株のコロニー形態は、野生株と同じく Rough 型であった（Fig. 1 A, C）。従って、本遺伝子（MSMEG2936 / Rv2609c 遺伝子）は、コロニー形態、すなわち細胞壁構造に影響を与えていることが示された。野生株と破壊株のゲノムを用いて、MSMEG2936 遺伝子に対応するプライマーで PCR 反応を行い電気泳動でバンドを確認した結果、野生株のゲノムをテンプレートにした場合には MSMEG2936 遺伝子の大きさに対応したバンドが検出され、破壊株では MSMEG2936 遺伝子にカナマイシン耐性カセット遺伝子を加えたサイズのバンドが得られた。従って、破壊株中では MSMEG2936 遺伝子中にカナマイシン耐性カセットが挿入されていることが確認された。

2. 細胞壁に関連した遺伝子を用いた抗酸菌の新規検出・鑑別法

本研究で作成したプライマー（結核菌のゲノム上で Rv3783 と Rv3789 遺伝子に対応）を用いて、結核菌、*M. avium*、*M. smegmatis*、及び *E. coli* のゲノムをテンプレートとして予想サイズ（結核菌：6.5 kbp、*M. avium*：3.1 kbp、*M. smegmatis*：3.7 kbp、及び *E. coli*：なし）にバンドが得られる PCR 反応条件の検討を行った結果、LA Taq ポリメラーゼ（TaKaRa）と添付のバッファーを用いた条件下で抗酸菌特異的に予想サイズにバンドが得られた（Fig2. A）。決定した条件で 18 種類の抗酸菌のコロニーをテンプレートとしたPCR反応を行い電気泳動で

バンドを確認した結果、*M. scrofulaceum* と *M. smegmatis*、*M. avium* と *M. intracellulare*、*M. kansasii* と結核菌がそれぞれ同じ位置に明確なバンドが検出された（Fig. 2 B）。一方、その他の抗酸菌をテンプレートとした場合には、明確なバンドは得られなかった（Fig. 2 B　一部の菌種は省略）。次ぎに、臨床分離株を含めた 12 菌種 84 株のコロニーをテンプレートとしたPCR反応と電気泳動を行った。その結果、新たに *M. rhodesiae* をテンプレートとした場合に2.5 kbpの位置に明確なバンドが見られることが示された。従って、本研究で設計したプライマーを用いれば、抗酸菌を、結核菌と *M. kansasii* のグループ、*M. avium* と *M. intracellulare*（MAC）のグループ、*M. smegmatis* と *M. scrofulaceum* のグループ、*M. rhodesiae*、及びそれ以外の５つに簡便に鑑別できることが示された。テンプレートとして使用した抗酸菌の菌種と今回行った鑑別法の結果が一致したのは94株、非一致は8株であった。非一致の 8 株について同定試験をやり直した結果、8株中 5 株については今回行った鑑別法の結果が正しいことが証明された。残りの 3 株については、使用した同定キットで明確な菌種の同定が出来なかった。従って、最終的に菌種と今回行った鑑別法は97%一致していた。

本鑑別法では、結核菌と *M. kansasii* が同じサイズのバンドとして検出されるため、結核菌を特異的に検出する条件の検討を行った。結核菌群に特異的な遺伝子、Rv3786c 遺伝子と Rv3783 遺伝子に対応するプライマーを用いて、上記と同様の PCR 条件下で PCR 反応と電気泳動を行った結果、ゲノムをテンプレートとした場合も、コロニーをテンプレートとした場合も結核菌群のみに明確なバンドが検出された。従って、結核菌群と *M. kansasii* を別々に鑑別出来ることが示された。そのため、本鑑別法により抗酸菌を簡便に、結核菌群、MAC、*M. kansasii*、*M. smegmatis* と *M. scrofulaceum* のグループ、*M. rhodesiae*、及びその他の６つのグループに鑑別出来ることが可能である。

D. 考察

M. smegmatis において MSMEG2936 遺伝子を破壊することによって、コロニー形態が大きく変化することから、MSMEG2936 遺伝子（結核菌では Rv2609c 遺伝子に相当）がコロニー形態、すなわち細胞壁構造に関与していることが示された（Fig. 1）。本破壊株中で結核菌由来の Rv2609c 遺伝子（MSMEG2936 遺伝子に相当）を発現させると、コロニー形態は野生株と同じ Rough 型になるため（Fig. 1）、Rv2609c 遺伝子も MSMEG2936 遺伝子と同様に細胞壁構造に関与していることが示された。本遺伝子は、抗酸菌における細胞壁成分の１つである、リポアラビノマンナンの生合成に関与していることが報告されている遺伝子群と同じオペロン上に存在していることから、本遺伝子もリポアラビノマンナンの生合成に関与していることが考えられる。リポアラビノマンナンの生合成経路に関しては未知の部分が多く残されており、本研究を進めることによってその一端が明らかにされることが期待される。

本研究で作成したプライマーを用いて PCR 反応と電気泳動を行うことにより、抗酸菌を簡便に、結核菌群、MAC、*M. kansasii*、*M. smegmatis* と *M. scrofulaceum* のグループ、*M. rhodesiae*、及びその他の６つのグループに鑑別出来ることが示された。臨床的に重要な抗酸菌は、結核菌、MAC、*M. kansasii* であり、本方法ではこれらを簡便に検出・鑑別することが可能である。抗酸菌の 16SrRNA の遺伝子情報を基にした PCR 反応による既存の簡易鑑別法は結核菌と MAC のみを判別するものであり、本方法はそれに加えてヒトに対して抗酸菌症を引き起こす *M. kansasii* も検出・鑑別できる点で優れていた。

E. 結論

M. smegmatis を用いて破壊株と相補株を作成することにより、MSMEG2936 遺伝子（結核菌では Rv2609c 遺伝子）が抗酸菌の細胞壁構造に関与していることを示した。本遺伝子はリポアラビノマンナンの生合成に関与していることが考えられる。

抗酸菌の細胞壁に関与する遺伝子を利用

することによって、抗酸菌を簡便に検出・鑑別することが可能であることを示した。本鑑別法は、既存の方法と比較して *M. kansasii* を鑑別出来る点で優れていた。

G. 研究発表

1. 論文発表

投稿準備中

2. 学会発表

発表準備中

H. 知的財産権の出願・登録状況

1. 特許取得　細胞壁に関与する遺伝子を用いた抗酸菌の新規検出・鑑別法について出願を準備している

2. 実用新案登録　なし

3. その他　なし

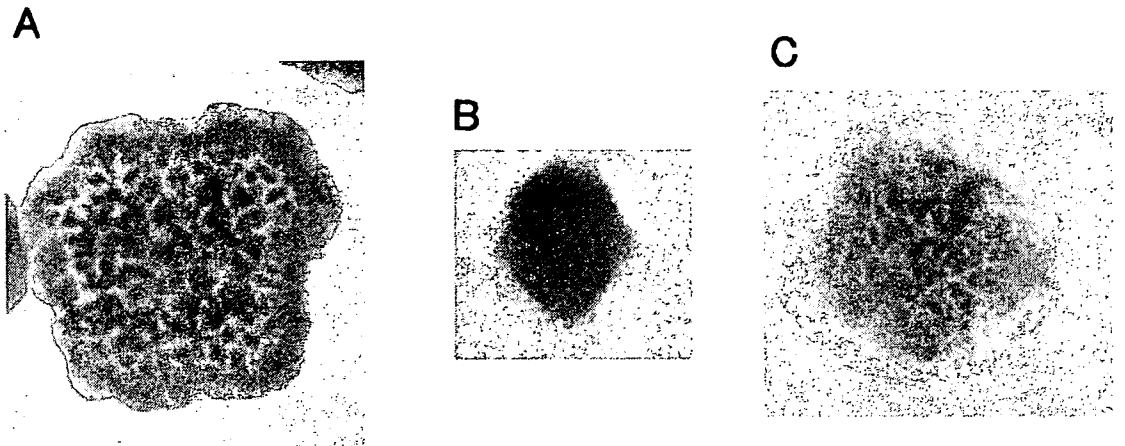

Fig. 1 コロニー形態　A. *M. smegmatis* 野生株、B. 破壊株（MSMEG2936 遺伝子）、C. 相補株（破壊株＋Rv2609c 遺伝子）

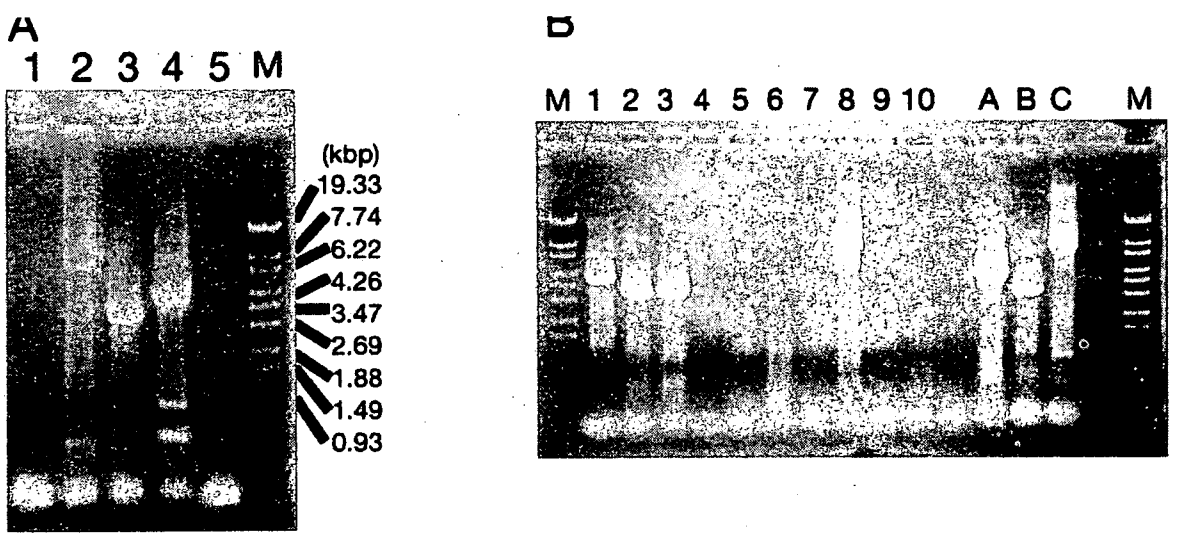

Fig.2 A ゲノムをテンプレートとした場合
1. ブランク、2. 結核菌、3. *M. avium*、4. *M. smegmatis*、5. *E. coli*、M. マーカー
B コロニーをテンプレートとした場合
1. *M. scrofulaceum*、2. *M. avium*、3. *M. intracellulare*、4. *M. marinum*、5. *M. xenopi*、6. *M. gordonae*、7. *M. abscessus*、8. *M. kansasii*、9. *M. szulgai*、10. *M. flavescens*、A. *M. smegmatis*、B. *M. avium*、C. 結核菌（A-C はゲノム）、M. マーカー

研究成果の刊行に関する一覧表

研究成果の刊行に関する一覧表

書籍

著者氏名	論文タイトル名	書籍全体の編集者名	書　籍　名	出版社名	出版地	出版年	ページ

雑誌

発表者氏名	論文タイトル名	発表誌名	巻号	ページ	出版年
T. Kaku, I. Kawamura, R. Uchiyama, T. Kurenuma M. Mitsuyama.	RD1 region in mycobacterial genome is involved in the induction of neciorss in infected RAW264 cells via mitochondrial membrane damage and ATP depletion	FEMS Microbiol. Lett.	274	189-195	2007
R. Uchiyama, I. Kawamura, T. Fujimura, M. Kawanishi, K. Tsuchiya, T. Tominaga, T. Kaku, Y. Fukasawa, S. Sakai, T. Nomura M. Mitsuyama.	Involvement of caspase-9 in the inhibition of necrosis of RAW 264 cells infected with *Mycobacterium tuberculosis.*	Infect. Immun.	75	2894-2902	2007
A. Bhatt, N. Fujiwara, K. Bhatt, S. S. Gurcha, L. Kremer, B. Chen, J. Chan, S. A. Porcelli, K. Kobayashi, G. S. Besra, W. R. Jacobs, Jr.	Deletion of *kasB* in *Mycobacterium tuberculosis* causes loss of acid-fastness and subclinical latent tuberculosis in immunocompetent mice.	Proc. Natl. Acad. Sci. USA	104	5157-5162	2007
T. Katsube, S. Matsumoto, M. Takatsuka, M. Okuyama, Y. Ozeki, M. Naito, Y. Nishiuchi, N. Fujiwara, M. Yoshimura, T. Tsuboi, M. Torii, N. Oshitani, T. Arakawa, K. Kobayashi.	Control of cell wall assembly by a histone-like protein in mycobacteria.	J. Bacteriol.	189	8241-8249	2007
I. Sugawara, Z. Li, L. Sun, T. Udagawa, T. Taniyama.	Recombinant BCG Tokyo (Ag 85A) protects cynomolgus mo nkeys (Macaca fascicularis) infected with H37Rv *Mycobacterium tuberculosis.*	Tuberculosis	87	518-525	2007

R. Shi, J. Zhang, K. Otomo, G. Zhang, I. Sugawara.	Lack of correlation between embB mutation and ethambutol minimal inhibitory concentration in *Mycobacterium tuberculosis* c linical isolates from China.	Antimicrob. Agents Chemother.	51	4515-4517	2007
H. Yamada, S. Mizuno, A. Ross, I. Sugawara.	Retinoic acid therapy attenuates the s everity of tuberculosis while a ltering lymphocyte and macrophage numbers and cytokine expression in rats infected with *M. tuberculosis*.	J. Nutr.	137	2696-2700	2007
R. Shi, J. Zhang, C. Li, Y. Kazumi, I. Sugawara.	Detection of streptomycin resistance in *Mycobacterium tuberculosis* clinical isolates from China as determined by denaturing HPLC analysis and DNA sequencing.	Microbes Infect.	9	1538-1544	2007
M. Makino, Y. Maeda, Y. Fukutomi, T. Mukai.	Contribution of GM-CSF on the enhancement of the T cell-stimulating activity of macrophages.	Microbes and Infect.	9	70-77	2007
Y. Maeda, T. Mukai, M. Kai, Y. Fukutomi, H. Nomaguchi , C. Abe , K. Kobayashi, S. Kitada, R, Maekura, I. Yano, N. Ishii, T. Mori, M. Makino.	Evaluation of major membrane protein-II as a tool for serodiagnosis of leprosy.	FEMS Microbiol. Lettr.	272	202-205	2007
M. Kai, Y. Fujita, Y. Maeda, N. Nakata, S. Izumi, I. Yano, M. Makino.	Identification of trehalose dimycolate (cord factor) in *Mycobacterium leprae*.	FEBS Lett.	581	3345-3350	2007
Y. Miyamoto, T. Mukai, Y. Maeda, N. Nakata, M. Kai, T. Naka, I. Yano, M. Makino.	Characterization of the fucosylation pathway in the biosynthesis of glycopeptidolipids from *Mycobacterium avium* comple x.	J. Bacteriol.	189	5515-5522	2007

M. S. Duthie, W. Goto, G. C. Ireton, S. T. Reece, L. P. V. Cardoso, C. M. T. Martelli, M. M. A. Stefani, M. Nakatani, R. C. de Jesus, E. M. Netto, M. V. F. Balagon, E. Tan, R. H. Gelber, Y. Maeda, M. Makino, D. Hoft, S. G. Reed.	Use of Protein Antigens for early serological diagnosis of leprosy.	Clin. Vaccine Immunol.	14	1400-1408	2007
A. J. Wolf, B. Linas, G. J. Trevejo-Nuñez, E. Kincaid, T. Tamura, K. Takatsu, J. D. Ernst.	*Mycobacterium tuberculosis* Infects dendritic cells with high frequency and impairs their function *in vivo*.	J. Immunol.	179	2509-2519	2007
H. Ariga, Y. Shimohakamada, M. Nakada, T. Tokunaga, T. Kikuchi, A. Kariyone, T. Tamura, K. Takatsu.	Instruction of naive $CD4^+$ T-cell fate to T-bet expression and T helper 1 development : roles of T-cell receptor-mediated signals.	Immunology	122	212-221	2007
I. Sugawara, H. Yamada, S. Mizuno.	BCG vaccination enhances resistance to *M. tuberculosis* infection in guinea pigs fed a low casein diet.	Tohoku J. Exp. Med.	in press		
K. Hibiya, Y. Kazumi, I. Sugawara, J. Fujita.	Histopathological classification of systemic *Mycobacterium avium* comple x infections in slaughtered domestic pigs.	Comp. Immunol. Microbiol. Infect. Dis.	in press		
A. J. Wolf, L. Desvignes, B. Linas, N. Banaiee, T. Tamura, K. Takatsu, J. D. Ernst.	Initiation of the adaptive immune response to *M. tuberculosis* depends on antigen production in the local lymph node, not the lungs.	J. Exp. Med.	in press		

河村伊久雄 光山正雄	抗結核防御免疫と結核菌による免疫制御	実験医学（羊土社）	25	3183-3189	2007
河村伊久雄	結核菌の病原性発現機構はどこまで判ったか	化学療法の領域	23	1750-1756	2007
松本壮吉、 尾関百合子、 小林和夫.	結核菌の新規病原因子 MDP1 の感染病態への関わり.	感染・炎症・免疫	37	98-101	2007
岡部真裕子、 大原直也、 小林和夫.	結核. 特集. 新興・再興感染症の現状と予防	保健の科学	49	691-697	2007

RD1 region in mycobacterial genome is involved in the induction of necrosis in infected RAW264 cells via mitochondrial membrane damage and ATP depletion

Taijin Kaku, Ikuo Kawamura, Ryosuke Uchiyama, Takeshi Kurenuma & Masao Mitsuyama

Department of Microbiology, Kyoto University Graduate School of Medicine, Kyoto, Japan

Correspondence: Ikuo Kawamura, Department of Microbiology, Kyoto University Graduate School of Medicine, Yoshidakonoe-cho, Sakyo-ku, Kyoto 606-8501, Japan. Tel.: +81 75 753 4447; fax: +81 75 753 4446; e-mail: ikuo_kawamura@mb.med.kyoto-u.ac.jp

Received 8 March 2007; accepted 30 May 2007.

DOI:10.1111/j.1574-6968.2007.00838.x

Editor: Peter Andrew

Keywords
Mycobacterium tuberculosis; necrosis; RD1; mitochondria; ATP; RAW264 cells.

Abstract

It was shown that virulent *Mycobacterium tuberculosis* H37Rv induces necrosis of infected RAW264 cells at 24 h post infection while avirulent H37Ra and an attenuated H37Rv mutant that is deficient for RD1 region (H37RvΔ*RD1*) cause less necrosis of the infected cells. While H37Rv caused damage of the mitochondrial inner membrane and decreased the level of intracellular ATP, H37RvΔ*RD1* did not exhibit these harmful effects in infected cells. On the other hand, there was no difference in the level of intracellular reactive oxygen species after infection with H37Rv or H37RvΔ*RD1*, and the intracellular bacterial numbers of H37RvΔ*RD1* and H37Ra were comparable to that of H37Rv. These results suggested that some virulence factors of H37Rv may contribute to the necrosis of infected cells through induction of mitochondrial dysfunction and depletion of intracellular ATP. RD1 appeared to encode some components possibly playing a central role in the induction of host cell necrosis after *M. tuberculosis* infection.

Introduction

Macrophages are the primary target cells in the host infected with *Mycobacterium tuberculosis* (MTB). After infection into the cells of a macrophage lineage, MTB survives and multiplies inside cells by blocking the bactericidal mechanisms such as phagosomal acidification and phagosome–lysosome fusion. Host cells that cannot control the intracellular bacterial growth appear to be a comfortable niche for MTB. In this regard, apoptotic destruction of the infected macrophages has been proposed as a host defense mechanism to inhibit the spread of the disease process (Bocchino *et al.*, 2005). However, Keane *et al.* (2000) showed that virulent MTB is capable of growing inside macrophages by inhibition of cellular apoptosis.A recent report has shown that virulent MTB has a greater ability to cause necrosis of infected cells rather than does avirulent MTB (Chen *et al.*, 2006). In contrast to apoptosis, necrosis does not affect the intracellular growth of MTB and may allow acceleration of bacterial growth outside the cells (Sly *et al.*, 2003). These data indicate that the ability for apoptosis inhibition and necrosis induction is highly related to the virulence of MTB. This supports the concept that necrosis of cells by MTB infection is a major factor contributing to the pathogenesis of the disease process; however, the mechanism remains to be elucidated further.

The mitochondrion is an important organelle not only for ATP synthesis but also for the regulation of cell death including both apoptosis and necrosis (Armstrong, 2006). Marzo *et al.* (1998) reported that a damage to the mitochondrial outer membrane causes the release of cytochrome *c*, followed by apoptosis of cells through apoptosome formation and caspase activation. On the other hand, Nakagawa *et al.* (2005) showed that cells undergo necrosis when the inner membrane of the mitochondria is injured. In the case of MTB infection, virulent H37Rv caused necrosis of the infected cells through damage to the mitochondrial inner membrane whereas avirulent H37Ra did not exert such an activity (Chen *et al.*, 2006). The result strongly suggests that some gene products involved in the mitochondrial membrane damage may exist exclusively in H37Rv but not in H37Ra.

Recently, Behr *et al.* (1999) identified 16 deletions in the mycobacterial genome (designated region of difference, RD) that were present in MTB but absent in avirulent *Mycobacterium bovis* BCG. Mostowy *et al.* (2004) have shown that

the expression of genes at the RD1 locus is reduced in H37Ra compared with that in H37Rv. Hsu *et al.* (2003) have shown that the deletion of RD1 attenuates the virulence of MTB, while the severity of necrosis at the site of infection is alleviated when compared with the wild type. These results suggest strongly that RD1 may be essential in the induction of necrosis in the cells infected with MTB. In this study, based on the above findings, the necrosis-inducing ability of H37Rv and the mutant defective for RD1 was compared, it was found that the RD1 is involved in the induction of necrosis of the infected macrophages mainly by inducing damage of the mitochondrial inner membrane and causing ATP depletion.

Materials and methods

Bacterial strains

MTB H37Rv, mutant H37Rv strain deficient for the RD1 region (H37RvΔ*RD1*) and the complemented strain H37RvΔ*RD1* (pYUB412::*Rv3860–Rv3885c*) were kindly provided by Dr Tsungda Hsu Jr (Howard Hughes Medical Institute, NY) (Hsu *et al.*, 2003). H37Ra has been maintained in the authors' laboratory. These MTB strains were grown at 37 °C to the mid-log phase in Middlebrook 7H9 broth supplemented with 0.5% albumin, 0.2% dextrose, 3 μg mL^{-1} catalase and 0.2% glycerol. Bacteria were harvested, stirred vigorously with glass beads and centrifuged at 300 *g* for 3 min to remove the bacterial clumps, and then stored at −80 °C in aliquots. After thawing, the absence of bacterial clumps in the suspension was confirmed by Kinyoun staining. The viability of bacteria was determined in each experiment by counting the colonies after plating the diluted suspension on Middlebrook 7H10 agar plates containing 50 μg mL^{-1} oleic acid, 0.5% albumin, 0.2% dextrose, 4 μg mL^{-1} catalase and 0.85 mg mL^{-1} sodium chloride.

Enumeration of intracellular bacteria

RAW264 cells were obtained from the Riken Cell Bank (Ibaraki, Japan) and maintained in RPMI1640 medium supplemented with 10% fetal bovine serum. Cells were seeded in a 12-well culture plate at 1×10^5 cells well^{-1} and incubated for 12 h at 37 °C in the culture medium, washed and infected with 1×10^6 CFU of bacteria for 4 h. After washes, cells were cultured for 24 h in the presence of 5 μg mL^{-1} gentamicin and lysed in 0.05% Triton X-100 solution. The number of viable bacteria was enumerated by plating the cell lysate on Middlebrook 7H10 agar plates and colony counting after incubation for 21 days.

Detection of necrosis by measuring the release of lactate dehydrogenase (LDH) and propidium iodide (PI) staining

RAW264 cells (10^5) were infected with each strain of MTB (10^6 CFU) as described above and the culture supernatants were collected on the constant interval during 24 h. To monitor the degree of necrosis of the infected cells, the amount of LDH released from the infected cells was measured using an LDH Cytotoxicity Detection Kit (Takara Bio Inc., Shiga, Japan). The percentage of LDH released was calculated according to the following formula: % release = 100 × (experimental LDH release − spontaneous LDH release)/(maximal LDH release − spontaneous LDH release). A value of maximal LDH release was obtained from the supernatant of cells treated with 0.5% Triton X-100. Alternatively, RAW264 cells (10^5) were infected with MTB (10^6 CFU) for 24 h and stained with 0.2 mM PI for 5 min on ice. After washes with phosphate buffered saline (PBS), cells were fixed in 1% paraformaldehyde for 15 min and a fluorescence image was captured.

Measurement of DNA fragmentation

To detect apoptosis, RAW264 cells (10^5) were infected with each strain of MTB (10^6 CFU) and lysed 24 h after infection. Oligonucleosomes in the lysate were quantified using a Cell Death Detection ELISA^{PLUS} (Roche, Diagnostics, Penzberg, Germany) according to the manufacturer's protocol. The degree of DNA fragmentation was expressed as an arbitrary unit calculated by the following formula: Arbitrary unit = ($A_{405\,nm}$ of experimental group − $A_{405\,nm}$ of negative control (medium alone))/($A_{405\,nm}$ of untreated cells − $A_{405\,nm}$ of negative control).

Flow cytometric analysis

RAW264 cells (10^5) were infected with MTB (10^6 CFU) for varying periods and stained with 0.1 nM 3, 3′-dihexyloxycarbocyanine iodide $DiOC_6(3)$ (Molecular Probe, Eugene, OR) that emits the fluorescence after accumulation in the mitochondria (Korchak *et al.*, 1982). Cells were detached from the culture plates, washed and suspended in PBS containing 0.2% albumin. If the inner membrane of the mitochondria is damaged after MTB infection, the mitochondria are not able to retain $DiOC_6(3)$ any longer, resulting in the loss of fluorescence. Based on this, the integrity of mitochondrial inner membrane was assessed by measuring the fluorescence emission using a FACSCalibur (Becton Dickinson, Tokyo, Japan). To monitor the generation of intracellular reactive oxygen species (ROS), RAW264 cells were infected with MTB for 3 h and incubated with 5 μM dichlorodihydrofluorescein diacetate (DCFH-DA), which penetrates into the cytoplasm and emits fluorescence

when converted into oxidized form by intracellular ROS (Bass *et al.*, 1983). After washes, the fluorescence intensity of the cells was determined using the FACSCalibur.

Measurement of ATP level

RAW264 cells were infected with MTB as described above, washed once with PBS and lysed in 0.5% trichloroacetic acid. The amount of ATP in the cell lysate was determined using an ENLITEN® ATP Assay System Bioluminescence Detection Kit (Promega Corporation, Madison, WI). Chemiluminescence was measured by an ARVO SX 1420 multilabel counter (PerkinElmer, Boston, MA). The chemiluminescence detected by this procedure could be taken as ATP derived from RAW 264 cells, as no positive result was recorded in a sample of MTB without cells. The relative amount of ATP was expressed as an arbitrary unit calculated by the following formula: %ATP level = 100 × (relative light unit (RLU) of the experimental group − RLU of negative control (medium alone))/(RLU of untreated cells − RLU of negative control).

Statistical analysis

Student's *t*-test was used to determine the statistical significance of the values obtained, and a P value of < 0.05 was considered to be statistically significant.

Results and discussion

RD1 is involved in the necrosis of MTB-infected RAW264 cells

It has been reported that virulent MTB strains cause less apoptosis of infected human cells but induce necrosis compared with avirulent MTB strains (Sly *et al.*, 2003). To confirm the virulence-associated cytolytic effect of MTB on murine macrophages, first, necrosis-inducing ability toward RAW264 murine macrophage-like cells between virulent MTB H37Rv and attenuated H37Ra strains was compared. Cells were infected for 24 h and the amount of LDH released in the culture supernatant was determined as a representative marker of necrosis. Similar to human macrophages, a significant level of LDH release was observed in the culture supernatant of H37Rv-infected cells but not in that of noninfected cells (Fig. 1a). The level of LDH release in the cells infected with H37Ra was substantially lower than that with H37Rv. It was confirmed that virulent H37Rv possesses a higher activity to cause necrosis in RAW264 cells than that of avirulent H37Ra.

Recent studies have shown that mutant H37Rv deficient for RD1 exhibits an attenuated virulence compared with H37Rv, and hardly induces necrosis of the lung in infected mice (Hsu *et al.*, 2003; Junqueira-Kipnis *et al.*, 2006).

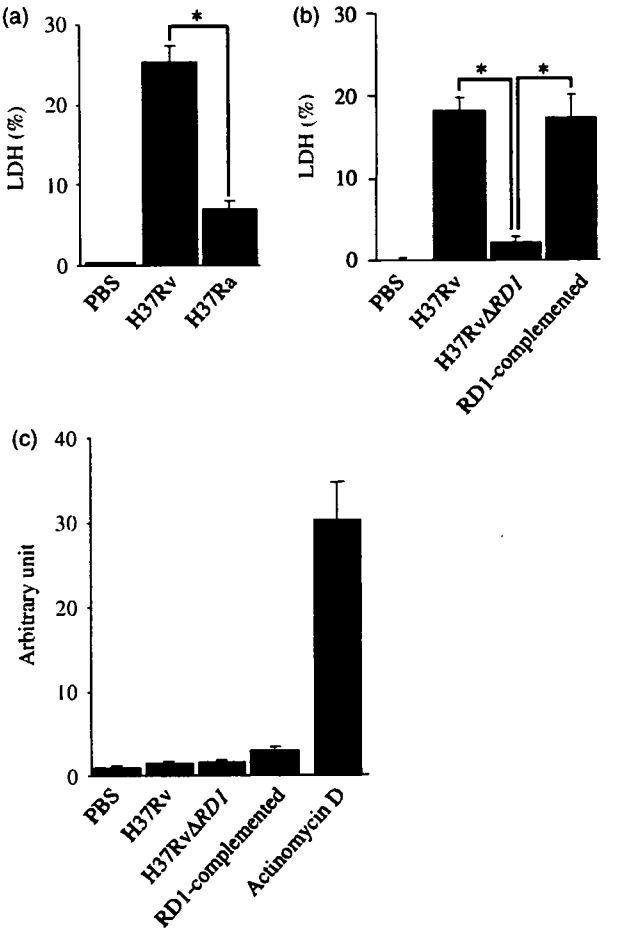

Fig. 1. LDH release and oligonucleosome formed in the cells infected with H37Rv, H37RvΔ*RD1* and RD1-complemented strains. RAW264 cells were infected with the MTB strains at MOI of 10 for 4 h and the amount of LDH was measured 24 h later. (a) LDH activity in the culture supernatant of cells infected with H37Rv and H37Ra. (b) LDH activity in the culture supernatant of cells infected with H37Rv, H37RvΔ*RD1* and RD1-complemented strains. (c) Cells were infected with H37Rv, H37RvΔ*RD1* and RD1-complemented strains, or incubated with 1 μg mL^{-1} actinomycin D for 24 h. The cell lysate was prepared and the amount of oligonucleosomes was determined. Data represent the mean ± SD of triplicate assays and are representative of three independent experiments.

Although the RD1 locus is also present in H37Ra, it has been shown that the expression of genes at RD1 is reduced when compared with that of H37Rv (Mostowy *et al.*, 2004). These findings prompted investigation of whether the RD1 of MTB is involved in the induction of necrosis in RAW264 cells after infection. To test this possibility, RAW264 cells were infected with H37Rv, H37RvΔ*RD1* and H37RvΔ*RD1* complemented with RD1 for 24 h, and LDH released in the supernatant was measured. As shown in Fig. 1b, a high level of LDH release was induced by H37Rv, but not by H37RvΔ*RD1*. As expected, the impaired activity of the deficient mutant to induce LDH release was restored by complementation with RD1.

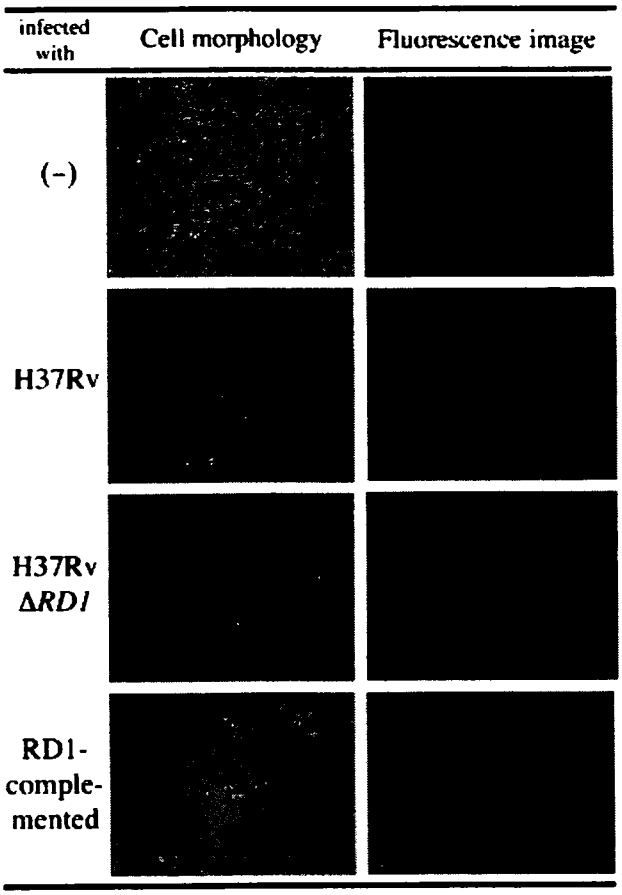

Fig. 2. PI staining of RAW264 cells infected with H37Rv, H37RvΔ*RD1* and RD1-complemented strains. RAW264 cells were infected with the MTB strains for 24 h and stained with PI. The cells were observed in bright field (left) and the fluorescence image was detected under UV excitation light (right). Data are representative of three independent experiments.

To rule out the possible contribution of apoptotic cell death to the LDH release, the amount of oligonucleosomes in the infected cells was quantified 24 h after infection with each MTB strain. Compared with the level of apoptosis induced by treatment with actinomycin D as a positive control, only a marginal increase was seen after infection, but there was no difference among three groups (Fig. 1c). Next, cells were stained with PI 24 h after infection to analyze the population of PI-stained cells using a fluorescence microscope. Under this experimental condition, there was no significant difference in the proportion of cells infected with bacteria among these three groups (data not shown). Most of the cells infected with H37Rv became PI-positive (Fig. 2). No PI-positive cell could be observed after infection with H37RvΔ*RD1*, and an image nearly similar to the infection with H37Rv was obtained in cells infected with the RD1-complemented strain of H37RvΔ*RD1*. This finding clearly indicated that the cell death induced by H37Rv was not due to apoptosis. The RD1 region of MTB appeared to be critically important for the induction of a necrosis type of host cell death upon infection.

RD1-dependent damage of the inner membrane of mitochondria in infected cells

It has been shown that H37Rv but not H37Ra injures the inner membrane of the mitochondria, resulting in the necrosis of infected macrophages (Chen *et al.*, 2006). In the present experiment, it was next examined whether H37Rv causes any damage to the mitochondria of RAW264 cells in a manner that depends on the presence of RD1. RAW264 cells were infected with H37Rv, H37RvΔ*RD1* and its RD1-complemented strain for 2–24 h, and stained with $DiOC_6(3)$ to assess the integrity of mitochondrial inner membrane. Noninfected cells showed a single-peaked profile due to the accumulation of fluorescent dye inside the inner membrane of the mitochondria. The shift of the profile to a lower intensity was regarded as the result of inner membrane damage, followed by the loss of dye accumulation. Compared with the intensity of uninfected cells, the peak of fluorescence was diverse. A similar change in the FACS profile was detected as early as 2 h after infection with H37Rv or H37RvΔ*RD1* complemented with RD1 (Fig. 3). At this time point, the cell population expressing lower fluorescence (M2) was 30% or 31% of the total cells infected with H37Rv or H37RvΔ*RD1*complemented with RD1, respectively. The population of the cells that lost an intact level of fluorescence was gradually increased during the 24 h (38% in H37Rv-infected cells and 55% in those infected with the RD1-complemented strain). Such a significant change was not observed in the cells infected with H37RvΔ*RD1*, and almost the same intact profile as in noninfected cells was maintained for 24 h after infection. To rule out the possibility that the significant differences observed between H37Rv and H37RvΔ*RD1* were simply due to the difference in the number of bacteria that infected and replicated intracellularly for 24 h, the number of bacteria during the culture period was compared. At the beginning of culture, there was no significant difference in the number of infected bacteria among all the groups (Table 1). The bacteria grew gradually and showed a similar growth rate during the 24-h culture. The values in fold-increase calculated at 24 h of culture for each group were 2.9, 2.5 and 2.1 for H37Rv, H37RvΔ*RD1* and H37RvΔ*RD1* complemented with RD1, respectively. Although there was some difference in the values expressed in the fold-increase, it was clear that the small difference in bacterial growth could never account for the significant level of difference in the cytotoxic effect observed in this study.

It has been shown that the RD1 locus contains genes coding for the components of the secretory machinery and two secretory molecules, designated as 'early secreted

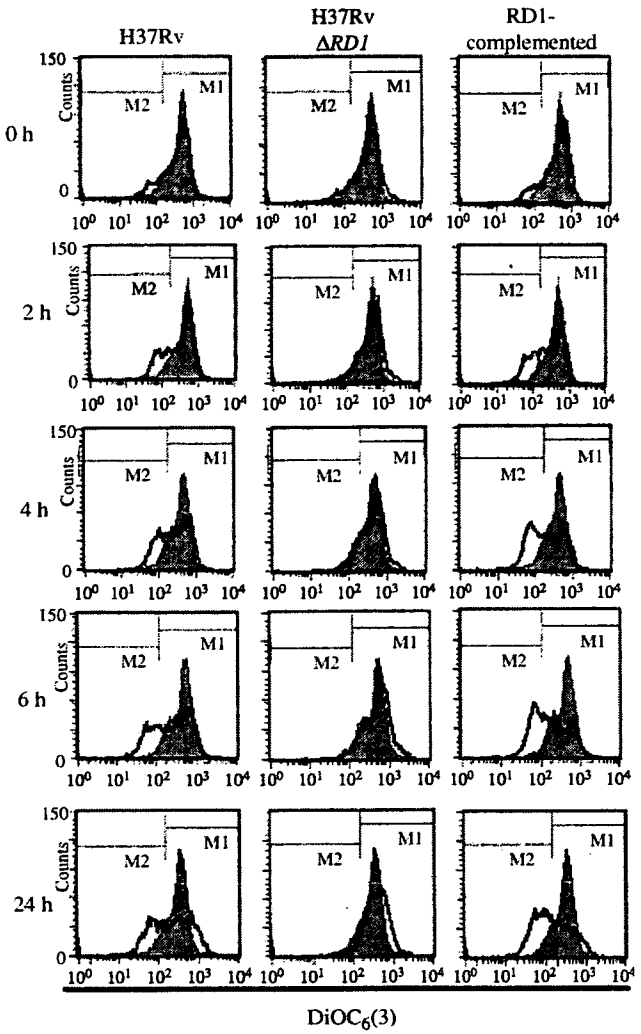

Fig. 3. Measurement of mitochondrial injury in RAW264 cells after infection with H37Rv, H37Rv*ΔRD1* and RD1-complemented strains. RAW264 cells were infected with the MTB strains at MOI of 10 for 4 h. Thereafter, cells were collected at the indicated times after infection and stained with $DiOC_6(3)$. The fluorescence intensity was measured by FACS. The shaded peak represents the fluorescence intensity of cells without infection. The bold line indicates the fluorescence profile of the MTB-infected cells. Data are representative of three independent experiments.

Table 1. Comparison of intracellular growth of H37Rv, H37Rv*ΔRD1* and RD1-complemented strain in RAW264 cells

	MTB ($\times 10^5$ CFU) well^{-1}*	
Bacteria	0 day	1 day
H37Rv	3.3 ± 0.5	9.6 ± 1.2
H37Rv*ΔRD1*	4.0 ± 0.1	9.8 ± 0.7
RD1-complemented	3.4 ± 1.4	7.3 ± 1.7

*RAW264 cells were infected with the MTB strains at MOI of 10 for 4 h. After washes, cells were lysed immediately (0 day) and 1 day after cultivation in 0.05% Triton X-100, and the CFU number was determined. Data represent the mean ± SD of triplicate assays and are representative of three independent experiments.

antigen of tuberculosis 6' (ESAT-6) and 'culture filtrate protein 10' (CFP-10) (Berthet *et al.*, 1998). It has been shown that ESAT-6 alone or in combination with CFP-10 may cause disintegration of the plasma membrane (Hsu *et al.*, 2003) and that some mycobacterial proteins are capable of penetrating through the phagosomal membrane in infected macrophages (Teitelbaum *et al.*, 1999). Thus, it is probable that ESAT-6 and CFP-10 may be secreted in the cytoplasm and contribute to the induction of mitochondrial membrane damage, whereas the expression of ESAT-6 and CFP-10 is reported to be downregulated in phagosome (Schnappinger *et al.*, 2003). Alternatively, it has been shown that the complex of these proteins binds specifically to the cell membrane of the macrophages (Renshaw *et al.*, 2005). The interaction of host cells with mycobacterial products may cause mitochondrial membrane damage; however, the more exact mechanism remains to be elucidated.

H37Rv infection causes depletion of ATP but does not affect generation of ROS in the cytoplasm

It has been shown that destruction of the mitochondrial inner membrane affects electron transport and oxidative phosphorylation, resulting in the depletion of ATP and an increase of ROS generation in the cytoplasm (Skulachev, 2006). A recent study also demonstrated that reduction of intracellular ATP level and an increase in intracellular ROS are the causes of necrotic cell death in infection with *Shigella flexneri* (Koterski *et al.*, 2005). Consequently, it was investigated whether intracellular ROS is generated by H37Rv infection and contributes to the induction of necrosis. RAW264 cells were infected with H37Rv, H37Rv*ΔRD1* and RD1-complemented strains, and the generation of intracellular ROS was evaluated by measuring the fluorescence intensity of DCFH-DA, an indicator for intracellular ROS. The three MTB strains similarly enhanced the fluorescence intensity 3 h after infection (Fig. 4a). Butylated hydroxyanisole (BHA), a scavenger of ROS, diminished these fluorescence emissions, indicating that a similar level of intracellular ROS was generated after infection with these MTB strains (Fig. 4b). However, H37Rv and H37Rv*ΔRD1* complemented with RD1 caused a decrease in the fluorescence of $DiOC_6(3)$ but H37Rv*ΔRD1* did not (Fig. 4c). Moreover, the shift of fluorescence peak was not restored by BHA while intracellular ROS was mostly abolished (Fig. 4d). It has been shown that overproduction of ROS by the mitochondria causes necrosis (Goossens *et al.*, 1995). However, Lee *et al.* (2006) reported that macrophages eventually undergo necrosis in response to a high intracellular burden of MTB without participation of intracellular ROS. Although ROS was detected after infection with H37Rv strains in this study, ROS was unlikely to be involved in the

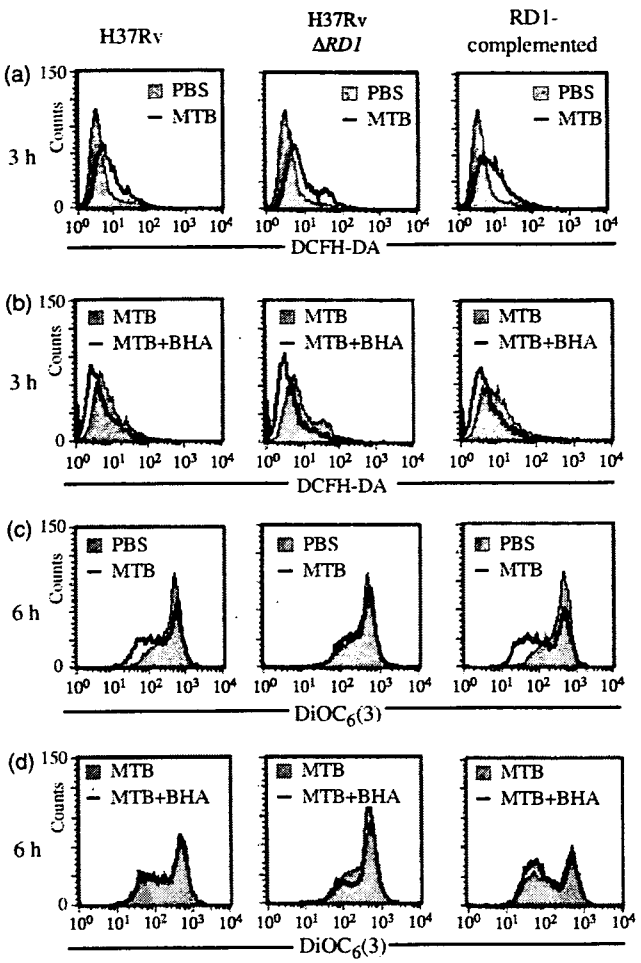

Fig. 4. Generation of ROS in RAW264 cells infected with H37Rv, H37Rv*ΔRD1* and RD1-complemented strains. RAW264 cells were infected with the MTB strains at an MOI of 10 for 3 h in the absence (a) or presence (b) of BHA. Cells were incubated with DCFH-DA and the fluorescence intensity was measured. RAW cells were infected with the MTB strains for 6 h in the absence (c) or presence (d) of BHA. Cells were incubated with $DiOC_6(3)$ and the fluorescence intensity was measured. Data are representative of three independent experiments.

mitochondrial injury of the infected cells. Therefore, it seems that MTB does not induce ROS generation by mitochondria.

Next, the amount of intracellular ATP was measured to examine whether the change in the intracellular ATP level plays a role in the necrosis of H37Rv-infected cells. Figure 5 clearly shows that the level of ATP was reduced by $< 50\%$ when cells were infected with H37Rv and an RD1-complemented strain for 6 h, but such a change was not observed when cells were infected with H37Rv*ΔRD1*. Kinetic study revealed that the decline in the ATP level was detected as early as 2 h after the infection and was maintained at least for 6 h (data not shown). The reduction of ATP did not appear to be due to the difference in the condition of bacteria, because RAW264 cells were infected with single

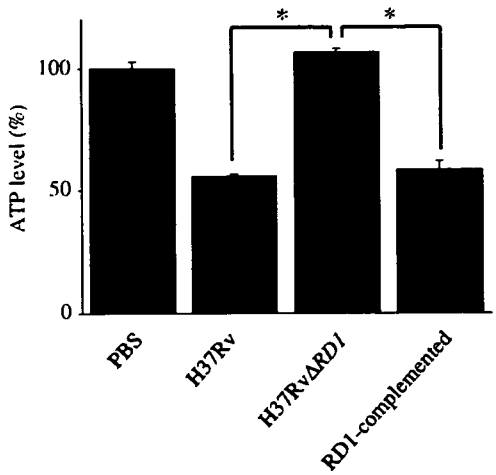

Fig. 5. Determination of intracellular ATP level in RAW264 cells infected with H37Rv, H37Rv*ΔRD1* and RD1-complemented strains. RAW264 cells were infected with the MTB strains at an MOI of 10 for 6 h and the level of intracellular ATP was determined. Data represent the mean ± SD of triplicate assays and are representative of three independent experiments.

cells of MTB strains that were highly viable. Koterski *et al.* (2005) showed that virulent *Shigella* caused a rapid reduction of the ATP level to about 50% and triggered necrosis of the infected macrophages. Therefore, it is likely that the change of ATP level may account for the necrosis of MTB-infected cells.

Taken together, the results presented in this study suggested strongly that H37Rv, a virulent strain of MTB, is capable of affecting the inner membrane of mitochondria resulting in the induction of necrotic-type death of host cells in a manner dependent on the RD1 locus. The RD1-dependent cellular necrosis appeared due to the depletion of intracellular ATP. The present study may have provided important findings that extend the understanding of the molecular mechanism involved in the pathology of infection with MTB.

Acknowledgements

This work was supported by a Grant-in-Aid for Scientific Research on Priority Areas from the Ministry of Education, Science, Culture and Sports of Japan, Grant-in-Aid for Scientific Research (B) and (C) from The Japan Society for the Promotion of Science and in part by a Grant-in Aid for Scientific Research from the Ministry of Health, Labor and Welfare, Japan.

References

Armstrong JS (2006) Mitochondrial membrane permeabilization: the sine qua non for cell death. *BioEssays* **28**: 253–260.

Bass DA, Parce JW, Dechatelet LR, Szejda P, Seeds MC & Thomas M (1983) Flow cytometric studies of oxidative product formation by neutrophils: a graded response to membrane stimulation. *J Immunol* **130**: 1910–1917.

Behr MA, Wilson MA, Gill WP, Salamon H, Schoolnik GK, Rane S & Small PM (1999) Comparative genomics of BCG vaccine by whole-genome DNA microarray. *Science* **284**: 1520–1523.

Berthet FX, Rasmussen PB, Rosenkrands I, Andersen P & Gicquel B (1998) A *Mycobacterium tuberculosis* operon encoding ESAT-6 and a novel low-molecular-mass culture filtrate protein (CFP-10). *Microbiology* **144**: 3195–3203.

Bocchino M, Galati D, Sanduzzi A, Colizzi V, Brunetti E & Mancino G (2005) Role of mycobacteria-induced monocyte/macrophage apoptosis in the pathogenesis of human tuberculosis. *Int J Tuberc Lung Dis* **9**: 375–383.

Chen M, Gan H & Remold HG (2006) A mechanism of virulence: *Mycobacterium tuberculosis* strain H37Rv, but not attenuated H37Ra, causes significant mitochondrial inner membrane disruption in macrophage leading to necrosis. *J Immunol* **176**: 3707–3716.

Goossens V, Grooten J, De Vos K & Fiers W (1995) Direct evidence for tumor necrosis factor-induced mitochondrial reactive oxygen intermediates and their involvement in cytotoxicity. *Proc Natl Acad Sci USA* **92**: 8115–8119.

Hsu T, Hingley-Wilson SM, Chen B *et al.* (2003) The primary mechanism of attenuation of Bacillus Calmette–Guérin is a loss of secreted lytic function required for invasion of lung interstitial tissue. *Proc Natl Acad Sci USA* **100**: 12420–12425.

Junqueira-Kipnis AP, Basaraba RJ, Gruppo V *et al.* (2006) Mycobacteria lacking the RD1 region do not induce necrosis in the lungs of mice lacking interferon-γ. *Immunology* **119**: 224–231.

Keane J, Remold HG & Kornfeld H (2000) Virulent *Mycobacterium tuberculosis* strains evade apoptosis of infected alveolar macrophages. *J Immunol* **164**: 2016–2020.

Korchak HM, Rich AM, Wilkenfeld C, Rutherford LE & Weissmann G (1982) A carbocyanine dye, $DiOC_6(3)$, acts as a mitochondrial probe in human neutrophils. *Biochem Biophys Res Commun* **108**: 1495–1501.

Koterski JF, Nahvi M, Venkatesan MM & Haimovich B (2005) Virulent *Shigella flexineri* causes damage to mitochondria and triggers necrosis in infected human monocyte-derived macrophages. *Infect Immun* **73**: 504–513.

Lee J, Remold HG, Ieong MH & Kornfeld H (2006) Macrophage apoptosis in response to high intracellular burden of *Mycobacterium tuberculosis* is mediated by a novel caspase-independent pathway. *J Immunol* **176**: 4267–4274.

Marzo I, Brenner C, Zamzami N, Susin SA, Buetner G, Brdiczka D, Remy R, Xie ZH, Reed JC & Kroemer G (1998) The permeability pore complex: a target for apoptosis regulation by caspases and Bcl-2-related proteins. *J Exp Med* **187**: 1261–1271.

Mostowy S, Cleto C, Sherman DR & Behr MA (2004) The *Mycobacterium tuberculosis* complex transcriptome of attenuation. *Tuberculosis* **84**: 197–204.

Nakagawa T, Shimizu S, Watanabe T, Yamaguchi O, Otsu K, Yamagata H, Inohara H, Kubo T & Tsujimoto Y (2005) Cyclophilin D-dependent mitochondrial permeability transition regulates some necrotic but not apoptotic cell death. *Nature* **434**: 652–658.

Renshaw PS, Lightbody KL, Veverka V *et al.* (2005) Structure and function of the complex formed by the tuberculosis virulence factors CFP-10 and ESAT-6. *EMBO J* **24**: 2491–2498.

Schnappinger D, Ehrt S, Voskuil MI *et al.* (2003) Transcriptional adaptation of *Mycobacterium tuberculosis* within macrophages: insights into the phagosomal environment. *J Exp Med* **198**: 693–704.

Skulachev VP (2006) Bioenergetic aspects of apoptosis, necrosis and mitoptosis. *Apoptosis* **11**: 473–485.

Sly LM, Hingley-Wilson SM, Reiner NE & McMaster WR (2003) Survival of *Mycobacterium tuberculosis* in host macrophages involves resistance to apoptosis dependent upon induction of antiapoptotic Bcl-2 family member Mcl-1. *J Immunol* **170**: 430–437.

Teitelbaum R, Cammer M, Maitland ML, Freitag NE, Condeelis J & Bloom BR (1999) Mycobacterial infection of macrophages results in membrane-permeable phagosomes. *Proc Natl Acad Sci USA* **96**: 15190–15195.

INFECTION AND IMMUNITY, June 2007, p. 2894–2902 Vol. 75, No. 6
0019-9567/07/$08.00+0 doi:10.1128/IAI.01639-06

Involvement of Caspase-9 in the Inhibition of Necrosis of RAW 264 Cells Infected with *Mycobacterium tuberculosis*▽

Ryosuke Uchiyama,[1] Ikuo Kawamura,[1]* Takao Fujimura,[2] Michiko Kawanishi,[1] Kohsuke Tsuchiya,[1] Takanari Tominaga,[1] Taijin Kaku,[1] Yutaka Fukasawa,[1] Shunsuke Sakai,[1] Takamasa Nomura,[1] and Masao Mitsuyama[1]

Department of Microbiology, Kyoto University Graduate School of Medicine, Kyoto 606-8501, Japan,[1] and Department of Dermatology, Kitasato University School of Medicine, Sagamihara 228-8555, Japan[2]

Received 11 October 2006/Returned for modification 22 November 2006/Accepted 24 March 2007

In order to know how caspases contribute to the intracellular fate of *Mycobacterium tuberculosis* and host cell death in the infected macrophages, we examined the effect of benzyloxycarbonyl-Val-Ala-Asp(OMe)-fluoromethane (z-VAD-fmk), a broad-spectrum caspase inhibitor, on the growth of *M. tuberculosis* H37Rv in RAW 264 cells. In the cells treated with z-VAD-fmk, activation of caspase-8, caspase-3/7, and caspase-9 was clearly suppressed, and DNA fragmentation of the infected cells was also reduced. Under this experimental condition, it was found that the treatment markedly inhibited bacterial growth inside macrophages. The infected cells appeared to undergo cell death of the necrosis type in the presence of z-VAD-fmk. We further found that z-VAD-fmk treatment resulted in the generation of intracellular reactive oxygen species (ROS) in the infected cells. By addition of a scavenger of ROS, the host cell necrosis was inhibited and the intracellular growth of H37Rv was significantly restored. Among inhibitors specific for each caspase, only the caspase-9-specific inhibitor enhanced the generation of ROS and induced necrosis of the infected cells. Furthermore, we found that severe necrosis was induced by infection with H37Rv but not H37Ra in the presence of z-VAD-fmk. Caspase-9 activation was also detected in H37Rv-infected cells, but H37Ra never induced such caspase-9 activation. These results indicated that caspase-9, which was activated by infection with virulent *M. tuberculosis*, contributed to the inhibition of necrosis of the infected host cells, presumably through suppression of intracellular ROS generation.

Tuberculosis caused by *Mycobacterium tuberculosis* is still a serious threat to human health at the global level. It has been estimated that one-third of the world's population are infected, and 8 million people develop active tuberculosis every year (15, 29). A number of studies have been carried out to identify the pathogenic determinants of *M. tuberculosis*, and various candidate molecules that may contribute to mycobacterial virulence have been reported (7). However, the molecular mechanisms for the virulence still remain unclear.

Macrophages play a role in the first line of host defense against bacterial infection by exerting microbicidal activity and contribute to the development of protective T cells as antigen-presenting cells through production of cytokines, including interleukin-12 (IL-12) and IL-18 (26). However, *M. tuberculosis* is capable of modulating such host response and survives inside macrophages (15). Therefore, some type of host response in the infected cell itself is necessary to control the replication of *M. tuberculosis* in the initial phase of infection. There are several reports indicating that induction of early death of infected cells is an important and alternative strategy for host defense against *M. tuberculosis*. For instance, it has been shown that macrophages go into apoptosis upon infection with *M. tuberculosis* in a caspase-dependent manner, resulting in the suppression of intracellular bacterial replication, and that arrest of macrophage apoptosis conversely enhances bacterial growth (22, 28). Furthermore, it has been reported that the apoptotic vesicles formed in the infected macrophages have an important role in transporting the mycobacterial antigen to dendritic cells and developing cellular immunity against *M. tuberculosis* (25). These results suggest that apoptosis of the infected cells constitutes an important part of the host resistance and affects the fate of intracellular *M. tuberculosis*. To date, the intracellular cascade of apoptosis has been characterized well and various caspases are known to be involved in apoptosis induction (21).

Caspases are synthesized as biologically inactive precursors and converted into active forms by sequential proteolytic cleavage. The activation process is regulated by various intracellular components and is under strict control. Upon apoptosis, which is a form of innate immunity against bacteria, however, it appears that *M. tuberculosis* exerts resistance by modification of the activation cascade of caspases in the cells where it resides. Sly et al. have recently reported that virulent *M. tuberculosis* strains cause less apoptosis than attenuated strains by induction of macrophage antiapoptotic *mcl-1* gene expression (28). Balcewicz-Sablinska et al. have also shown that *M. tuberculosis* H37Rv inhibits apoptosis of infected macrophages by IL-10-dependent release of a soluble tumor necrosis factor (TNF) receptor that inactivates TNF-α (2). These findings suggest that though apoptosis is coupled with killing of intracellular *M. tuberculosis*, the bacterium possesses a virulence-associated ability to evade apoptosis.

In addition to apoptosis, it has been shown that *M. tubercu-*

* Corresponding author. Mailing address: Department of Microbiology, Kyoto University Graduate School of Medicine, Yoshidakonoe-cho, Sakyo-ku, Kyoto 606-8501, Japan. Phone: 81-75-753-4447. Fax: 81-75-753-4446. E-mail: ikuo_kawamura@mb.med.kyoto-u.ac.jp.

▽ Published ahead of print on 2 April 2007.

losis triggers necrosis of infected macrophages. Unlike apoptosis, it appears that necrosis does not interfere with the survival of intracellular *M. tuberculosis*. Moreover, it is supposed that *M. tuberculosis* ultimately escapes macrophages by inducing necrosis, and necrotic cell death provides the nutrient source for *M. tuberculosis* in granuloma (30). Park et al. have shown that virulent clinical strains rapidly grow inside macrophages and induce necrosis of infected macrophages (20). Hsu et al. have demonstrated that an attenuated mutant of *M. tuberculosis* H37Rv failed to induce necrosis of infected macrophages (14). These results suggest that virulence of *M. tuberculosis* is associated with the ability to manipulate not only apoptosis but also necrosis of infected macrophages. However, little is known about the regulatory mechanism of apoptosis and necrosis or the relationship between *M. tuberculosis*-induced caspase activation and the fate of intracellular bacteria.

In this study, we employed various caspase inhibitors and examined their effects on the intracellular growth of a virulent H37Rv strain in macrophage-like RAW 264 cells. Unexpectedly, it was found that inhibition of caspases resulted in the necrosis of H37Rv-infected cells and our analysis revealed that the activation of caspase-9 is involved critically in the inhibition of necrosis. Furthermore, we found that H37Ra did not induce either necrosis of infected cells or activation of caspase-9. It was suggested that virulent *M. tuberculosis* strains avoid excessive necrosis of infected host cells by inducing caspase-9 activation.

MATERIALS AND METHODS

Reagents. Benzyloxycarbonyl-Val-Ala-Asp(OMe)-fluoromethane (z-VAD-fmk; an inhibitor of various caspases) and acetyl-Tyr-Val-Ala-Asp-chloromethane (a caspase-1 inhibitor) were purchased from Peptide Institute, Inc. (Osaka, Japan). Other inhibitors, including benzyloxycarbonyl-Val-Asp(OMe)-Val-Ala-Asp(OMe)-fluoromethane (a caspase-2 inhibitor), benzyloxycarbonyl-Asp-(OMe)-Gln-Met-Asp(OMe)-fluoromethane (a caspase-3 inhibitor), benzyloxycarbonyl-Ile-Glu(OMe)-Thr-Asp(OMe)-fluoromethane (a caspase-8 inhibitor), benzyloxycarbonyl-Leu-Glu(OMe)-His-Asp(OMe)-fluoromethane (a caspase-9 inhibitor), and benzyloxycarbonyl-Phe-Ala-fluoromethylketone (z-FA-fmk; an inactive caspase inhibitor analogue), were purchased from Sigma Aldrich (St. Louis, MO), Merck Biosciences, Inc. (San Diego, CA), Techne Corporation (Minneapolis, MN), R & D Systems, Inc. (Minneapolis. MN), and Calbiochem (San Diego, CA), respectively. 3(2)-*t*-Butyl-4-hydroxyanisole (BHA) and 2',7'-dichlorodihydrofluorescein diacetate (DCFH-DA) were obtained from Wako Pure Chemical Industries (Osaka, Japan) and Molecular Probes (Eugene, OR), respectively. Rabbit anti-mouse caspase-9 antibody was obtained from Cell Signaling Technology, Inc. (Danvers, MA).

Bacteria. The *M. tuberculosis* H37Rv and H37Ra strains maintained in our laboratory were grown at 37°C to mid-log phase in Middlebrook 7H9 broth (Becton Dickinson Microbiology Systems, Sparks, MD) supplemented with 0.5% albumin, 0.2% dextrose, 3 μg/ml catalase, and 0.2% glycerol. H37Rv was harvested and stirred vigorously with glass beads to disperse the bacterial clumps and stood for 30 min. An upper part of the suspension without visible clumps was collected and stored at −80°C in aliquots. After being thawed, the bacterial suspension was centrifuged at 150 × *g* for 3 min to remove clumps, and only the upper part of the suspension was used for the experiments to ensure an even infection of each cell. Viable bacteria were enumerated by plating the diluted suspension on Middlebrook 7H10 agar plates containing 50 μg/ml oleic acid, 0.5% albumin, 0.2% dextrose, 4 μg/ml catalase, and 0.85 mg/ml sodium chloride and counting the number of colonies 3 weeks after incubation at 37°C.

Measurement of intracellular bacterial growth. RAW 264 cells were seeded in 24-well microplates at 1.0×10^5 cells/well and incubated for 12 h at 37°C in 5% CO_2 in a culture medium consisting of RPMI 1640 medium supplemented with 10% fetal bovine serum and 5 μg/ml of gentamicin. Cells were washed and infected with 5×10^5 CFU of H37Rv for 4 h. After three washes with the culture medium for removal of extracellular bacteria, the cells were cultured for 7 days in the presence or absence of various caspase inhibitors and/or BHA. Cells were lysed in 0.05% Triton X-100 solution, and the number of viable bacteria in each well was determined by plating the lysate on Middlebrook 7H10 agar plates. In one experiment, thioglycolate-induced peritoneal macrophages (1.0×10^5 cells) were infected with H37Rv and the intracellular bacterial number was determined 7 days later.

Detection of DNA fragmentation. Two days after infection at a multiplicity of infection (MOI) of 5, 5×10^6 cells were lysed in a lysis buffer consisting of 10 mM Tris-HCl (pH 7.6), 0.15 M NaCl, 5 mM $MgCl_2$, and 0.5% Triton X-100. Intact nuclei were collected by centrifugation at 1,000 × *g* for 5 min, suspended in 10 mM Tris-HCl (pH 7.6) buffer containing 0.4 M NaCl, 1 mM EDTA, and 1% Triton X-100, and centrifuged at 12,000 × *g* for 15 min to segregate the nucleoplasm from high-molecular-weight chromatin. The semipurified nucleoplasm was consecutively incubated at 37°C with 20 μg/ml of RNase for 1 h and 100 μg/ml of proteinase K for 2 h. DNA was extracted with the phenol-chloroform method and electrophoresed on a 1.4% agarose gel. After being stained with ethidium bromide, DNA was visualized on a UV transilluminator. Alternatively, oligonucleosomes were quantified by using a Cell Death Detection ELISA^{PLUS} kit (Roche Diagnostics, Penzberg, Germany) according to the manufacturer's protocol. The degree of DNA fragmentation was expressed as an arbitrary unit calculated by the following formula: arbitrary unit = (A_{405} of experimental group − A_{405} of negative control [medium only])/(A_{405} of untreated cells − A_{405} of negative control).

Flow cytometric analysis. RAW 264 cells were collected 2 and 4 days after infection and washed with phosphate-buffered saline (PBS) containing 0.2% albumin. Cells were incubated with 0.2 mM propidium iodide (PI; Molecular Probes, Eugene, OR) for 10 min on ice in the dark, washed, and fixed with 1% paraformaldehyde in PBS. Fluorescence intensity was analyzed by FACSCalibur (BD Biosciences, San Jose, CA). In order to detect intracellular reactive oxygen species (ROS), RAW 264 cells infected with H37Rv 2 days before were incubated with 5 μM DCFH-DA for 15 min at 37°C. DCFH-DA diffused into cells and was hydrolyzed to DCFH (2', 7'-dichlorohydrofluorescein). Cells were detached from culture plates, and the fluorescence intensity of DCFH, which was converted into oxidized form by intracellular ROS, was analyzed by FACSCalibur according to a method described previously (3).

Detection of LDH. RAW 264 cells and peritoneal macrophages were infected with H37Rv or H37Ra, and the culture supernatants were collected 2 and 4 days later. The amount of lactate dehydrogenase (LDH) released from the infected cells was measured using an LDH cytotoxicity detection kit (TaKaRa BIO Inc., Shiga, Japan). The percentage of LDH release was calculated according to the following formula: percent release = 100 × (experimental LDH release − spontaneous LDH release)/(maximal LDH release − spontaneous LDH release). A value for maximal LDH release was obtained from the supernatant of cells treated with 1% Triton X-100.

Transmission electron microscopy. RAW 264 cells were infected with H37Rv for 3 days. The cells were washed twice with PBS and once with 0.1 M cacodylic acid buffer and fixed with 2.5% glutaraldehyde in 0.1 M cacodylic acid buffer. After fixation, the cells were treated with 2% osmium tetroxide in 0.1 M cacodylic acid buffer, dehydrated by treatment with graded ethanol solutions, and embedded in Quetol-812 resin mixture-embedding media. The ultrathin sections were stained with uranyl acetate and lead citrate and examined with a JEOL model JEM-1200EX electron microscope. The percentage of cells undergoing apoptosis or necrosis was estimated by investigating the morphologies of 100 cells in each experimental group.

Measurement of caspase activities. RAW 264 cells were lysed 1 and 2 days after infection, and the caspase-8, caspase-3 and/or -7, and caspase-9 activities in the cleared lysate were measured by using Caspase-Glo 8, Caspase-Glo 3/7, and Caspase-Glo 9 assays (Promega Corporation, Madison, WI) according to the manufacturer's protocols.

Statistical analysis. Student's *t* test was used to determine the statistical significance of the values obtained, and *P* values of <0.05 were considered statistically significant.

RESULTS

Effect of z-VAD-fmk on intracellular growth of H37Rv. In order to determine the effect of inhibition of caspase activities on the intracellular growth of H37Rv in RAW 264 cells, we first infected the cells with H37Rv at an MOI of 5 in the presence or absence of z-VAD-fmk and monitored the number of intracellular bacteria. H37Rv replicated slowly in RAW 264 cells in the absence of z-VAD-fmk (Fig. 1). A similar pattern of

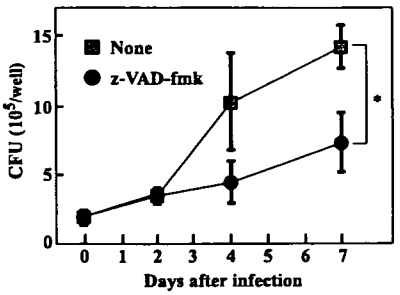

FIG. 1. Kinetics of intracellular growth of H37Rv in RAW 264 cells treated with or without z-VAD-fmk. RAW 264 cells were infected with H37Rv at an MOI of 5 and cultured in the presence or absence of 40 μM z-VAD-fmk. Cells were lysed at the indicated days, and the number of viable bacteria was determined by a CFU assay. Data represent the means ± standard deviations for triplicate assays and are representative of three independent experiments. *, $P < 0.05$.

growth was observed in z-VAD-fmk-treated macrophages for 2 days after infection. However, the growth rate was suppressed afterwards. To rule out the possibility that the growth inhibition is due to the direct action of z-VAD-fmk on H37Rv, we incubated H37Rv (5×10^5 CFU) in Middlebrook 7H9 broth including albumin, dextrose, and catalase for 7 days in the presence or absence of z-VAD-fmk and recovered 1.52×10^7 CFU or 1.56×10^7 CFU of H37Rv from the culture, respectively. A similar result was observed when H37Rv was cultured in the cell culture medium (data not shown). The results showed that z-VAD-fmk by itself did not influence bacterial growth and raised the possibility that some initiator and/or effector caspases were involved in facilitating the intracellular survival of H37Rv. Several studies clearly showed that caspase-8 and caspase-9 (initiator caspases) and caspase-3 (an effector caspase) are activated after *M. tuberculosis* infection and cause cell death in infected macrophages (22). Thus, we speculated that these caspases might have some activity influencing the fate of intracellular bacteria. To make this point clear, we examined whether these caspases were activated after infection with H37Rv and whether z-VAD-fmk inhibited the activation. As shown in Fig. 2, a significant level of caspase-8 activation was observed 1 day after infection and the activity decreased back to the control level by 2 days. The activities of caspase-3/7 and caspase-9 were increased on day 2 about four- and twofold, respectively. These caspase activities were at the control level on day 5, indicating that H37Rv induced activation of caspases to some extent. On the other hand, H37Rv-induced activations of these caspases were mostly inhibited in the presence of z-VAD-fmk and were not affected by z-FA-fmk (an inactive caspase inhibitor analogue). Since growth inhibition of the intracellular bacteria was detected in z-VAD-fmk-treated cells later than 2 days after infection, the results suggest that caspases may play a role in the intracellular survival of virulent *M. tuberculosis*.

z-VAD-fmk treatment causes necrosis of infected RAW 264 cells. To find the reason z-VAD-fmk treatment inhibited bacterial growth, on day 3 of infection, infected cells in the presence or absence of z-VAD-fmk were examined under an electron microscope. We did not detect any morphological change between normal cells (Fig. 3A) and cells treated only with z-VAD-fmk for 3 days (Fig. 3B). However, we found that infection of RAW 264 cells with H37Rv influenced cell morphology. Among the infected cells, 42% of the cells maintained their cellular structures (Fig. 3C and D) and 26% showed apoptotic structural changes (Fig. 3E). The remaining 32% of the cells displayed morphological changes characteristic of necrosis (Fig. 3F). The treatment with z-VAD-fmk provoked

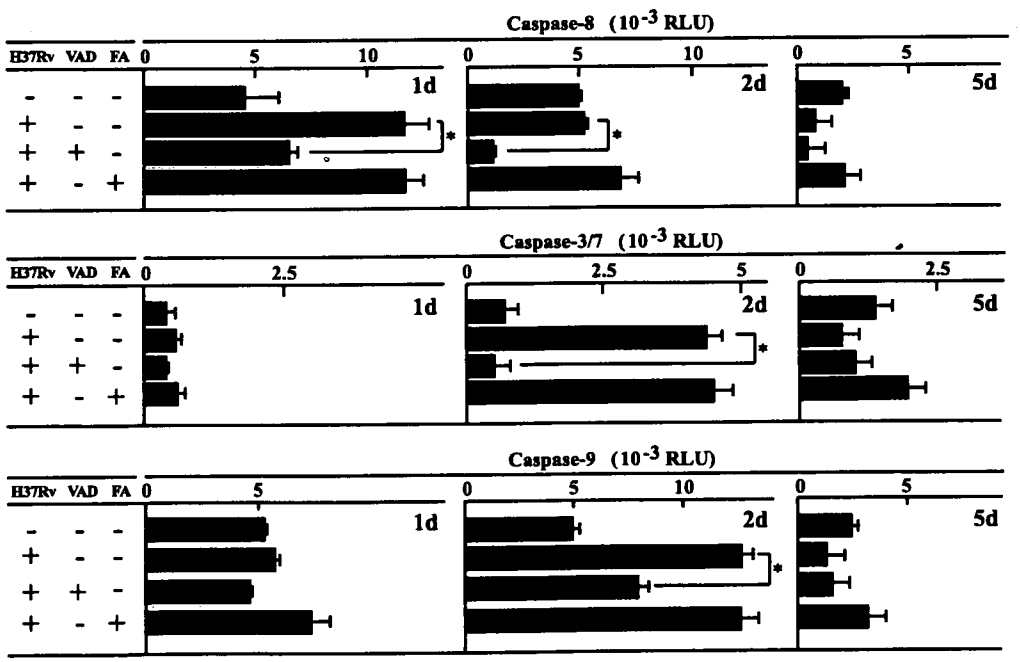

FIG. 2. Caspase activities after infection with H37Rv. RAW 264 cells were infected with H37Rv, and caspase activities were measured at 1, 2, and 5 days after infection by a Caspase-Glo assay. VAD, z-VAD-fmk; FA, z-FA-fmk; RLU, relative light units. Data represent the means ± standard deviations for triplicate assays and are representative of three independent experiments. *, $P < 0.05$.

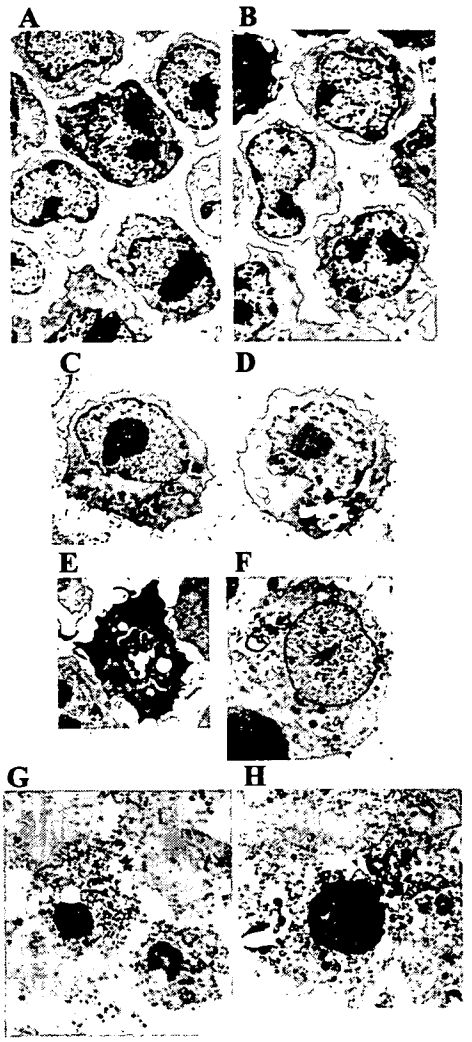

FIG. 3. Effect of z-VAD-fmk on morphologies of infected cells. RAW 264 cells infected with H37Rv were cultured for 3 days in the absence (C to F) or presence (G, H) of z-VAD-fmk. Cells were fixed, and morphologies were observed under an electron microscope. (E) A representative apoptotic cell. (F) A cell showing necrotic damage. (C and D) Infected cells which maintained normal cell morphologies. (A and B) Nontreated cells (A) and cells treated only with z-VAD-fmk (B). Micrographs were taken at magnifications of ×5,000 (A to F and H) and ×3,000 (G).

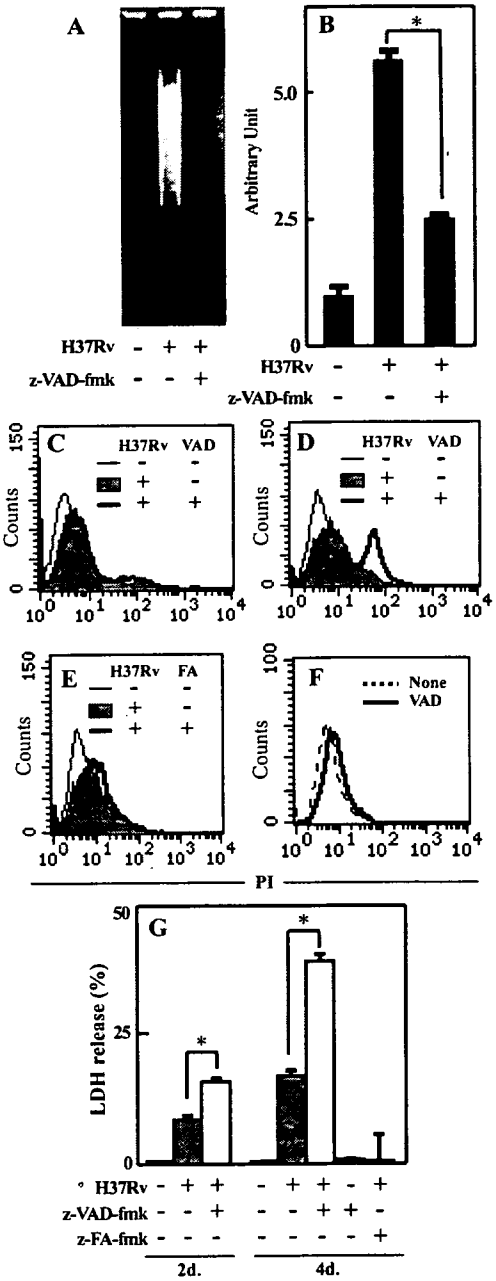

FIG. 4. Inhibition of apoptosis and induction of necrosis by z-VAD-fmk treatment. RAW 264 cells were infected with H37Rv and cultured for 2 days. Cells were lysed, and the DNA ladder and oligonucleosomes were detected by agarose gel electrophoresis (A) and quantified by an enzyme-linked immunosorbent assay (B), respectively. Two days (C) and 4 days (D, E) after infection, the cells were stained with PI and fluorescence intensity was measured. VAD, z-VAD-fmk; FA, z-FA-fmk. (F) Fluorescence intensity of the cells treated only with z-VAD-fmk for 4 days. (G) Culture supernatants were collected 2 and 4 days after infection, and LDH activity was assayed. Data represent the means ± standard deviations for triplicate assays and are representative of three independent experiments. *, $P < 0.05$.

much severe damage in the infected cells. As shown in Fig. 3G and H, the caspase inhibitor caused necrotic morphological changes in as many as 95% of the infected cells. These results raised the possibility that some caspases contribute to inhibition of necrosis of infected cells in conventional infection in vitro. To confirm that the morphological changes resulted from apoptosis or necrosis of the infected cells, we investigated a generation of oligonucleosomes and assessed the membrane integrity of the infected cells by measuring the population of PI-stained cells and LDH release into the culture medium. As shown in Fig. 4A, an oligonucleosomal DNA ladder was observed in RAW 264 cells infected with H37Rv but not in uninfected cells. Treatment with z-VAD-fmk clearly inhibited the cleavage of DNA. To analyze the DNA fragmentation quantitatively, the cell lysates were subjected to a sandwich enzyme-linked immunosorbent assay specific for oligonucleosomes. The number of oligonucleosomes in H37Rv-infected cells was about 5 times as high as that in the uninfected cells, but z-VAD-fmk significantly inhibited the generation of oligo-